Belle Preprint 2020-08
KEK Preprint 2020-07

Evidence for $X(3872) \to J/\psi\pi^+\pi^-$ produced in single-tag two-photon interactions

Y. Teramoto,[66] S. Uehara,[19,15] M. Masuda,[86,72] I. Adachi,[19,15] H. Aihara,[87] S. Al Said,[80,39] D. M. Asner,[3] H. Atmacan,[7] T. Aushev,[21] R. Ayad,[80] V. Babu,[8] P. Behera,[28] C. Beleño,[14] J. Bennett,[52] V. Bhardwaj,[25] B. Bhuyan,[26] T. Bilka,[5] J. Biswal,[35] G. Bonvicini,[92] A. Bozek,[62] M. Bračko,[49,35] T. E. Browder,[18] M. Campajola,[33,57] D. Červenkov,[5] M.-C. Chang,[10] P. Chang,[61] V. Chekelian,[50] A. Chen,[59] B. G. Cheon,[17] K. Chilikin,[44] K. Cho,[41] S.-J. Cho,[94] S.-K. Choi,[16] Y. Choi,[78] S. Choudhury,[27] D. Cinabro,[92] S. Cunliffe,[8] G. De Nardo,[33,57] F. Di Capua,[33,57] Z. Doležal,[5] T. V. Dong,[11] S. Eidelman,[4,65,44] T. Ferber,[8] B. G. Fulsom,[67] R. Garg,[68] V. Gaur,[91] N. Gabyshev,[4,65] A. Garmash,[4,65] A. Giri,[27] P. Goldenzweig,[36] D. Greenwald,[82] C. Hadjivasiliou,[67] T. Hara,[19,15] O. Hartbrich,[18] K. Hayasaka,[64] H. Hayashii,[58] M. T. Hedges,[18] M. Hernandez Villanueva,[52] W.-S. Hou,[61] C.-L. Hsu,[79] T. Iijima,[56,55] K. Inami,[55] G. Inguglia,[31] A. Ishikawa,[19,15] R. Itoh,[19,15] M. Iwasaki,[66] Y. Iwasaki,[19] W. W. Jacobs,[29] E.-J. Jang,[16] S. Jia,[11] Y. Jin,[87] C. W. Joo,[37] K. K. Joo,[6] J. Kahn,[36] A. B. Kaliyar,[81] K. H. Kang,[43] G. Karyan,[8] Y. Kato,[55] T. Kawasaki,[40] H. Kichimi,[19] C. Kiesling,[50] B. H. Kim,[74] D. Y. Kim,[77] S. H. Kim,[74] Y.-K. Kim,[94] T. D. Kimmel,[91] K. Kinoshita,[7] P. Kodyš,[5] S. Korpar,[49,35] D. Kotchetkov,[18] P. Križan,[45,35] R. Kroeger,[52] P. Krokovny,[4,65] T. Kuhr,[46] R. Kulasiri,[38] R. Kumar,[71] K. Kumara,[92] A. Kuzmin,[4,65] Y.-J. Kwon,[94] K. Lalwani,[48] J. S. Lange,[12] I. S. Lee,[17] S. C. Lee,[43] P. Lewis,[2] L. K. Li,[7] Y. B. Li,[69] L. Li Gioi,[50] J. Libby,[28] K. Lieret,[46] Z. Liptak,[23] D. Liventsev,[92,19] T. Luo,[11] C. MacQueen,[51] T. Matsuda,[53] D. Matvienko,[4,65,44] M. Merola,[33,57] K. Miyabayashi,[58] H. Miyata,[64] G. B. Mohanty,[81] S. Mohanty,[81,90] T. J. Moon,[74] T. Mori,[55] M. Mrvar,[31] R. Mussa,[34] E. Nakano,[66] M. Nakao,[19,15] H. Nakazawa,[61] Z. Natkaniec,[62] A. Natochii,[18] M. Nayak,[83] N. K. Nisar,[3] S. Nishida,[19,15] K. Ogawa,[64] S. Ogawa,[84] H. Ono,[63,64] Y. Onuki,[87] P. Pakhlov,[44,54] G. Pakhlova,[21,44] S. Pardi,[33] H. Park,[43] S.-H. Park,[94] S. Patra,[25] S. Paul,[82,50] T. K. Pedlar,[47] R. Pestotnik,[35] L. E. Piilonen,[91] T. Podobnik,[45,35] V. Popov,[21] E. Prencipe,[22] M. T. Prim,[36] M. Ritter,[46] A. Rostomyan,[8] N. Rout,[28] G. Russo,[57] D. Sahoo,[81] Y. Sakai,[19,15] S. Sandilya,[7] A. Sangal,[7] L. Santelj,[45,35] T. Sanuki,[85] V. Savinov,[70] G. Schnell,[1,24] J. Schueler,[18]

C. Schwanda,[31] Y. Seino,[64] K. Senyo,[93] M. E. Sevior,[51] M. Shapkin,[32] V. Shebalin,[18] J.-G. Shiu,[61] J. B. Singh,[68] E. Solovieva,[44] M. Starič,[35] Z. S. Stottler,[91] M. Sumihama,[13] K. Sumisawa,[19,15] T. Sumiyoshi,[89] W. Sutcliffe,[2] M. Takizawa,[75,20] U. Tamponi,[34] F. Tenchini,[8] M. Uchida,[88] T. Uglov,[44,21] Y. Unno,[17] S. Uno,[19,15] P. Urquijo,[51] Y. Usov,[4,65] R. Van Tonder,[2] G. Varner,[18] A. Vinokurova,[4,65] V. Vorobyev,[4,65,44] E. Waheed,[19] C. H. Wang,[60] E. Wang,[70] M.-Z. Wang,[61] P. Wang,[30] X. L. Wang,[11] M. Watanabe,[64] E. Won,[42] X. Xu,[76] B. D. Yabsley,[79] S. B. Yang,[42] H. Ye,[8] J. Yelton,[9] J. H. Yin,[42] Z. P. Zhang,[73] V. Zhilich,[4,65] V. Zhukova,[44] and V. Zhulanov[4,65]

(The Belle Collaboration)

[1]*University of the Basque Country UPV/EHU, 48080 Bilbao*

[2]*University of Bonn, 53115 Bonn*

[3]*Brookhaven National Laboratory, Upton, New York 11973*

[4]*Budker Institute of Nuclear Physics SB RAS, Novosibirsk 630090*

[5]*Faculty of Mathematics and Physics, Charles University, 121 16 Prague*

[6]*Chonnam National University, Gwangju 61186*

[7]*University of Cincinnati, Cincinnati, Ohio 45221*

[8]*Deutsches Elektronen–Synchrotron, 22607 Hamburg*

[9]*University of Florida, Gainesville, Florida 32611*

[10]*Department of Physics, Fu Jen Catholic University, Taipei 24205*

[11]*Key Laboratory of Nuclear Physics and Ion-beam Application (MOE) and Institute of Modern Physics, Fudan University, Shanghai 200443*

[12]*Justus-Liebig-Universität Gießen, 35392 Gießen*

[13]*Gifu University, Gifu 501-1193*

[14]*II. Physikalisches Institut, Georg-August-Universität Göttingen, 37073 Göttingen*

[15]*SOKENDAI (The Graduate University for Advanced Studies), Hayama 240-0193*

[16]*Gyeongsang National University, Jinju 52828*

[17]*Department of Physics and Institute of Natural Sciences, Hanyang University, Seoul 04763*

[18]*University of Hawaii, Honolulu, Hawaii 96822*

[19]*High Energy Accelerator Research Organization (KEK), Tsukuba 305-0801*

[20]*J-PARC Branch, KEK Theory Center,*
High Energy Accelerator Research Organization (KEK), Tsukuba 305-0801
[21]*Higher School of Economics (HSE), Moscow 101000*
[22]*Forschungszentrum Jülich, 52425 Jülich*
[23]*Hiroshima Institute of Technology, Hiroshima 731-5193*
[24]*IKERBASQUE, Basque Foundation for Science, 48013 Bilbao*
[25]*Indian Institute of Science Education and Research Mohali, SAS Nagar, 140306*
[26]*Indian Institute of Technology Guwahati, Assam 781039*
[27]*Indian Institute of Technology Hyderabad, Telangana 502285*
[28]*Indian Institute of Technology Madras, Chennai 600036*
[29]*Indiana University, Bloomington, Indiana 47408*
[30]*Institute of High Energy Physics,*
Chinese Academy of Sciences, Beijing 100049
[31]*Institute of High Energy Physics, Vienna 1050*
[32]*Institute for High Energy Physics, Protvino 142281*
[33]*INFN - Sezione di Napoli, 80126 Napoli*
[34]*INFN - Sezione di Torino, 10125 Torino*
[35]*J. Stefan Institute, 1000 Ljubljana*
[36]*Institut für Experimentelle Teilchenphysik,*
Karlsruher Institut für Technologie, 76131 Karlsruhe
[37]*Kavli Institute for the Physics and Mathematics of the Universe (WPI),*
University of Tokyo, Kashiwa 277-8583
[38]*Kennesaw State University, Kennesaw, Georgia 30144*
[39]*Department of Physics, Faculty of Science,*
King Abdulaziz University, Jeddah 21589
[40]*Kitasato University, Sagamihara 252-0373*
[41]*Korea Institute of Science and Technology Information, Daejeon 34141*
[42]*Korea University, Seoul 02841*
[43]*Kyungpook National University, Daegu 41566*
[44]*P.N. Lebedev Physical Institute of the Russian Academy of Sciences, Moscow 119991*
[45]*Faculty of Mathematics and Physics,*
University of Ljubljana, 1000 Ljubljana

[46]*Ludwig Maximilians University, 80539 Munich*

[47]*Luther College, Decorah, Iowa 52101*

[48]*Malaviya National Institute of Technology Jaipur, Jaipur 302017*

[49]*University of Maribor, 2000 Maribor*

[50]*Max-Planck-Institut für Physik, 80805 München*

[51]*School of Physics, University of Melbourne, Victoria 3010*

[52]*University of Mississippi, University, Mississippi 38677*

[53]*University of Miyazaki, Miyazaki 889-2192*

[54]*Moscow Physical Engineering Institute, Moscow 115409*

[55]*Graduate School of Science, Nagoya University, Nagoya 464-8602*

[56]*Kobayashi-Maskawa Institute, Nagoya University, Nagoya 464-8602*

[57]*Università di Napoli Federico II, 80126 Napoli*

[58]*Nara Women's University, Nara 630-8506*

[59]*National Central University, Chung-li 32054*

[60]*National United University, Miao Li 36003*

[61]*Department of Physics, National Taiwan University, Taipei 10617*

[62]*H. Niewodniczanski Institute of Nuclear Physics, Krakow 31-342*

[63]*Nippon Dental University, Niigata 951-8580*

[64]*Niigata University, Niigata 950-2181*

[65]*Novosibirsk State University, Novosibirsk 630090*

[66]*Osaka City University, Osaka 558-8585*

[67]*Pacific Northwest National Laboratory, Richland, Washington 99352*

[68]*Panjab University, Chandigarh 160014*

[69]*Peking University, Beijing 100871*

[70]*University of Pittsburgh, Pittsburgh, Pennsylvania 15260*

[71]*Punjab Agricultural University, Ludhiana 141004*

[72]*Research Center for Nuclear Physics, Osaka University, Osaka 567-0047*

[73]*Department of Modern Physics and State Key*
Laboratory of Particle Detection and Electronics,
University of Science and Technology of China, Hefei 230026

[74]*Seoul National University, Seoul 08826*

[75]*Showa Pharmaceutical University, Tokyo 194-8543*

[76] *Soochow University, Suzhou 215006*

[77] *Soongsil University, Seoul 06978*

[78] *Sungkyunkwan University, Suwon 16419*

[79] *School of Physics, University of Sydney, New South Wales 2006*

[80] *Department of Physics, Faculty of Science, University of Tabuk, Tabuk 71451*

[81] *Tata Institute of Fundamental Research, Mumbai 400005*

[82] *Department of Physics, Technische Universität München, 85748 Garching*

[83] *School of Physics and Astronomy,*

Tel Aviv University, Tel Aviv 69978

[84] *Toho University, Funabashi 274-8510*

[85] *Department of Physics, Tohoku University, Sendai 980-8578*

[86] *Earthquake Research Institute, University of Tokyo, Tokyo 113-0032*

[87] *Department of Physics, University of Tokyo, Tokyo 113-0033*

[88] *Tokyo Institute of Technology, Tokyo 152-8550*

[89] *Tokyo Metropolitan University, Tokyo 192-0397*

[90] *Utkal University, Bhubaneswar 751004*

[91] *Virginia Polytechnic Institute and State University, Blacksburg, Virginia 24061*

[92] *Wayne State University, Detroit, Michigan 48202*

[93] *Yamagata University, Yamagata 990-8560*

[94] *Yonsei University, Seoul 03722*

Abstract

We report the first evidence for $X(3872)$ production in two-photon interactions by tagging either the electron or the positron in the final state, exploring the highly virtual photon region. The search is performed in $e^+e^- \to e^+e^- J/\psi\pi^+\pi^-$, using 825 fb^{-1} of data collected by the Belle detector operated at the KEKB e^+e^- collider. We observe three $X(3872)$ candidates with an expected background of 0.11 ± 0.10 events, with a significance of 3.2σ. We obtain an estimated value for $\tilde{\Gamma}_{\gamma\gamma}\mathcal{B}(X(3872) \to J/\psi\pi^+\pi^-)$ assuming the Q^2 dependence predicted by a $c\bar{c}$ meson model, where $-Q^2$ is the invariant mass-squared of the virtual photon. No $X(3915) \to J/\psi\pi^+\pi^-$ candidates are found.

PACS numbers: 14.40.Gx, 13.25.Gv, 13.66.Bc

The charmonium-like state $X(3872)$ has been observed in various reactions since its first observation in $B \to KJ/\psi\pi^+\pi^-$ decays [1]. Its spin, parity, and charge conjugation were determined to be 1^{++} [2], but its internal structure is still a puzzle [3, 4]. Subsequent to the spin-parity determination, the $X(3872)$ has not been searched for in two-photon interactions because axial-vector particles are forbidden to decay to two real photons [5]. However, it has been pointed out that mesons with $J^{PC} = 1^{++}$ could be produced if one or both photons are highly virtual [6]—denoted as γ^*.

We have performed the first search for the production of the $X(3872)$ by two photons, using $e^+e^- \to e^+e^- X(3872)$, where one of the final-state electrons, referred to as a tagging electron, is observed, and the other scatters at an extremely forward (backward) angle and is not detected [7]. Such events are called single-tag events. The $X(3872)$ is reconstructed via its decay to $J/\psi\pi^+\pi^-$ ($J/\psi \to \ell^+\ell^-$). The two-photon decay width, which is obtained from this measurement, is sensitive to the internal structure of the $X(3872)$. Early attempts to calculate such decay widths for charmonium-like exotic states have been reported in Ref. [8]. The measurement reported here gives new insight to the $X(3872)$ puzzle. We also search for the $X(3915)$ in the same final state, $J/\psi\pi^+\pi^-$, through the G-parity-violating $J/\psi\rho^0$ ($\rho^0 \to \pi^+\pi^-$) channel, as well as $J/\psi\omega$ ($\omega \to \pi^+\pi^-$) decay[9].

We use 825 fb^{-1} of data collected by the Belle detector operated at the KEKB e^+e^- asymmetric collider [10, 11]. The data were taken at the $\Upsilon(nS)$ resonances ($n \leq 5$) and nearby energies, 9.43 GeV$< \sqrt{s} <$ 11.03 GeV. Of these data, 636 fb^{-1} are at, or 60 MeV

below, the $\Upsilon(4S)$ resonance.

The Belle detector is a general-purpose magnetic spectrometer, asymmetrically enclosing the e^+e^- interaction point [12, 13]. Charged-particle momenta are measured by a silicon vertex detector and a cylindrical drift chamber. Electron and charged-pion identification relies on a combination of the drift chamber, time-of-flight scintillation counters, aerogel Cherenkov counters, and an electromagnetic calorimeter made of CsI(Tl) crystals. Muon identification relies on the drift chamber and 14 layers of resistive plate chambers in the iron return yoke.

For Monte Carlo (MC) simulations, used to set selection criteria and derive the reconstruction efficiency, we use TREPSBSS [14, 15] to generate single-tag $e^+e^- \to e^+e^-X(3872)$ events in which the $X(3872)$ decays to $J/\psi\pi^+\pi^-$ and J/ψ decays leptonically. For simulating radiative J/ψ decays, we use PHOTOS [16, 17]. A GEANT3-based program simulates the detector response to these events [18].

Since one final-state electron is not detected, we select events with exactly five charged tracks, each coming from the interaction point (IP) and having $p_{\rm T} > 0.1$ GeV/c, with two or more having $p_{\rm T} > 0.4$ GeV/c, where $p_{\rm T}$ is the transverse momentum with respect to the e^+ direction.

J/ψ candidates are reconstructed by their decays to e^+e^- or $\mu^+\mu^-$ pairs. A charged track is identified as an electron (muon) from the J/ψ decay if its electron (muon) likelihood ratio is greater than 0.66 [19, 20][21] The invariant mass of the lepton pair is required to be in the range 3.047–3.147 GeV/c^2. In the calculation of the invariant mass of an e^+e^- pair, we include the four-momenta of radiated photons, having energy less than 0.2 GeV and angle relative to an electron direction of less than 0.04 radians.

The tagging electron must have an electron likelihood ratio greater than 0.95 or E/p greater than 0.87, where E is the energy measured by the electromagnetic calorimeter and p is the momentum of the particle. We require that the tagging electron have momentum above 1 GeV/c and $p_{\rm T} > 0.4$ GeV/c. The electron momentum includes the momenta of radiated photons, using the same requirements as for the electrons from J/ψ decays.

We identify a charged track as a pion if its kaon likelihood ratio is less than 0.8, its muon likelihood ratio is less than 0.9, its electron likelihood ratio is less than 0.6, and its E/p is less than 0.8 [22]. We require that events do not have any photons with energy above 0.4 GeV or any π^0 candidates whose χ^2 value in the mass constrained fit is less than 4.0.

As the $X(3872)$ should be back-to-back with the tagging electron projected in the plane perpendicular to the e^+e^- beam axis, we require the difference between their azimuthal angles be in the range $(\pi \pm 0.1)$ radians.

We require that the total visible transverse momentum of the event, $p^*_{\rm T}$ [23], be less than 0.2 GeV/c. We also require that the measured energy of the $J/\psi\pi^+\pi^-$ system, $E^*_{\rm obs}$, be consistent with the expectation, $E^*_{\rm exp}$, calculated from the observed momentum of the tagging electron and the direction and invariant mass of the $J/\psi\pi^+\pi^-$ system, imposing energy-momentum conservation. Since the energy and total transverse momentum are correlated, we impose a two-dimensional selection criterion

$$(p^*_{\rm T} + 40\ {\rm MeV}/c)\left(\left|\frac{E^*_{\rm obs} - E^*_{\rm exp}}{E^*_{\rm exp}}\right| + 0.003\right) < 3\ {\rm MeV}/c. \qquad (1)$$

Figure 1 shows the distribution of events and these selection criteria in the $p^*_{\rm T}$ vs. $E^*_{\rm obs}/E^*_{\rm exp}$ plane.

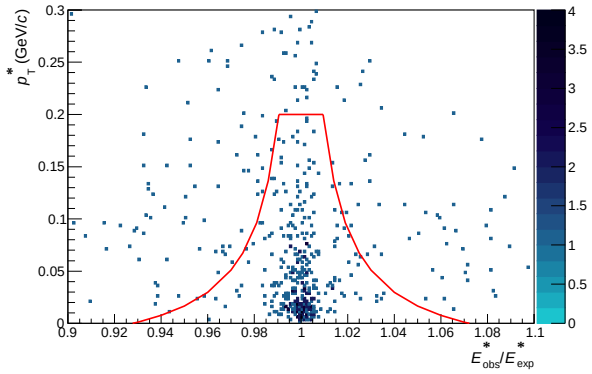

FIG. 1. $p^*_{\rm T}$ vs. $E^*_{\rm obs}/E^*_{\rm exp}$ distribution from data. The (red) line shows the selection criteria applied to $p^*_{\rm T}$ and $E^*_{\rm obs}/E^*_{\rm exp}$; events below the line are accepted.

Finally, we place a requirement on the missing momentum of the event, which is equal to the momentum of the unmeasured electron that goes down the beam pipe. We require the missing-momentum projection in the e^- beam direction in the center-of-mass frame be less than -0.4 GeV/c for e^--tagging events and greater than 0.4 GeV/c for e^+-tagging events.

We search for the $X(3872)$ and $X(3915)$ by looking for events in the $J/\psi\pi^+\pi^-$ invariant mass distribution, $M(J/\psi\pi^+\pi^-)$. The reconstructed mass resolution is expected to be 2.5 MeV/c^2 from the MC simulation. We define two signal regions: 3.867–3.877 GeV/c^2

for the $X(3872)$ and 3.895–3.935 GeV/c^2 for the $X(3915)$. The former accommodates the $X(3872)$ with the known mass of 3871.69 ± 0.17 MeV/c^2 and the small decay width of less than 1.2 MeV [24]; the latter accommodates the $X(3915)$ with the known mass of 3918.4 ± 1.9 MeV/c^2 and the larger decay width of 20 ± 5 MeV. We constrain the J/ψ mass to 3.09690 GeV/c^2 when we calculate $M(J/\psi\pi^+\pi^-)$ [25].

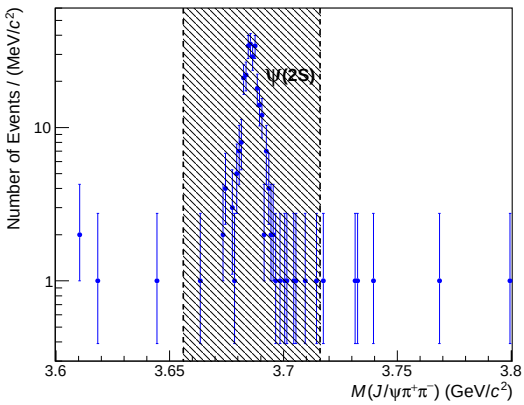

FIG. 2. $M(J/\psi\pi^+\pi^-)$ distribution shown with the $\psi(2S)$ veto (shaded gray region).

The dominant background, centered at 3.686 GeV/c^2, arises from radiatively produced $\psi(2S)$, $e^+e^- \to e^+e^-\psi(2S)$, with $\psi(2S) \to J/\psi\pi^+\pi^-$. Figure 2 shows the $M(J/\psi\pi^+\pi^-)$ distribution in data in the vicinity of $\psi(2S)$. Although the width of the $\psi(2S)$ peak is 2.7 MeV/c^2, its tail extends to the high-mass side. This feature was also seen in previous studies of initial-state-radiation (ISR) production of $J/\psi\pi^+\pi^-$ [26]. To remove $\psi(2S)$ events, we veto events within 0.03 GeV/c^2 of the $\psi(2S)$ mass, 3.686 GeV/c^2. Figure 3 shows the Q^2 distribution after removing those events, where $Q^2 = 2(p_{\rm in} \cdot p_{\rm out} - m_e^2c^2)$ with $p_{\rm in}$ and $p_{\rm out}$ being the four-momenta of the incoming (beam) and outgoing (tagging) electrons and m_e being the electron mass. In Fig. 3, data are dominated by background events while MC is pure $X(3872)$. Since two-photon processes are strongly suppressed at high Q^2, we require $Q^2 < 25$ GeV^2/c^2 to suppress non-two-photon background. Our measurement is insensitive for $Q^2 < 1.5$ GeV^2/c^2 due to a drop in reconstruction efficiency.

Figure 4 shows the observed events in the Q^2 vs. $M(J/\psi\pi^+\pi^-)$ plane. Three events are in the $X(3872)$ signal region; no events are in the $X(3915)$ region. The masses of the three events in the $X(3872)$ signal region are 3.8726, 3.8701 and 3.8742 GeV/c^2, giving the

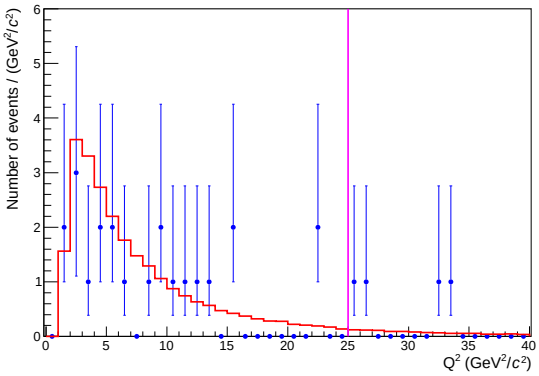

FIG. 3. Q^2 distribution for data (blue dots) and MC (red histogram). The area of MC distribution is normalized to that of data. The vertical (magenta) line indicates the applied selection requirement.

averaged mass of 3.8723±0.0012 GeV/c^2, where the uncertainty is statistical. At masses below the $X(3872)$ region, 3.716-3.867 GeV/c^2, there are six events, presumably from $\psi(2S)$ events; at masses above, there are no events below 4.266 GeV/c^2, in region of the $Y(4260)$ mass. A similar distribution was seen in the Belle ISR study [26], suggesting that the main cause of our background is t-channel photon-exchange processes with an emission of a single virtual photon that converts to the hadronic state.

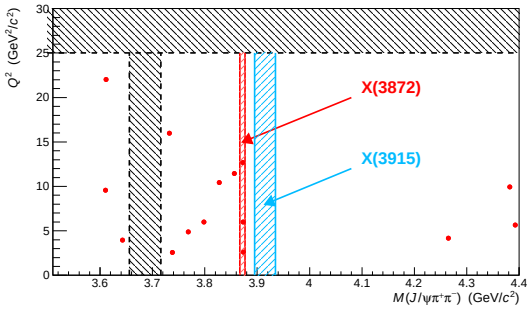

FIG. 4. Observed events (red dots) in the Q^2 vs. $M(J/\psi\pi^+\pi^-)$ plane. Three events are seen in the $X(3872)$ signal region (red lines with shade). The blue lines with shade show the $X(3915)$ signal region. The vetoed regions are shaded gray with dash lines.

To estimate the background level in the $X(3872)$ signal region, we fit a linear function

$$\max(0, a[M(J/\psi\pi^+\pi^-) - 3.872\ \text{GeV}/c^2] + b) \tag{2}$$

to the data in the mass region of ± 0.156 GeV/c^2 centered at the mass of the $X(3872)$, excluding the signal region; a and b are free parameters of the fit. The width of 0.156 GeV/c^2 is determined by the distance between the $X(3872)$ and the upper boundary, 3.716 GeV/c^2, of the $\psi(2S)$ vetoed region. Using an unbinned extended maximum-likelihood fit, we obtain $a = -345 \pm 195$ /(GeV/c^2)^2 and $b = 10.5 \pm 10.1$ /(GeV/c^2). This gives 0.11 ± 0.10 background events in the $X(3872)$ signal region, where the uncertainty is statistical only. By comparing this result to that from the power function, $a'/[M(J/\psi\pi^+\pi^-) - b']^{c'}$ with b' fixed at 2.4 GeV/c^2, we estimate the systematic uncertainty to be ± 0.01 events. Combining the statistical and systematic uncertainties in quadrature, we estimate 0.11 ± 0.10 background events.

With this background, the significance of three events is 3.2σ. For the $X(3872)$ signal, with three observed and 0.11 expected background events, we calculate the number of signal events, $N_{\rm sig} = 2.9^{+2.2}_{-2.0}(\text{stat.}) \pm 0.1(\text{syst.})$, using the Feldman-Cousins method [27] at 68% confidence level (C.L.). For the $X(3915)$ signal, with zero observed and 0.3 expected background events, $N_{\rm sig} < 2.14$ at 90% C.L.

The differential cross section for the production of a resonance (X) in a single-tag two-photon interaction is expressed as [28]

$$\frac{\mathrm{d}\sigma_{ee}(X)}{\mathrm{d}Q^2} = 4\pi^2 \left(1 + \frac{Q^2}{M^2}\right) \frac{2J+1}{M^2} \Gamma_{\gamma^*\gamma}(Q^2) \times 2 \left.\frac{\mathrm{d}^2 L_{\gamma^*\gamma}}{\mathrm{d}W \mathrm{d}Q^2}\right|_{W=M}, \quad (3)$$

where $L_{\gamma^*\gamma}$ is the single-tag luminosity function, M is the resonance mass, $-Q^2$ is the invariant mass squared of the virtual photon, $\Gamma_{\gamma^*\gamma}(Q^2)$ is the $\gamma^*\gamma$ decay width for the resonance, W is the invariant mass of the $\gamma^*\gamma$ system, and J is the resonance spin. The factor of two comes from the existence of two production modes: $e^-\gamma^*$ and $e^+\gamma^*$ scattering.

For a J=1 resonance, spin-parity conservation forbids production at $Q^2 = 0$. To remove the Q^2-dependence from $\Gamma_{\gamma^*\gamma}(Q^2)$, we use the reduced $\gamma\gamma$ decay width $\tilde{\Gamma}_{\gamma\gamma}$ defined as [6, 29]

$$\tilde{\Gamma}_{\gamma\gamma} \equiv \lim_{Q^2 \to 0} \frac{M^2}{Q^2} \Gamma^{\rm LT}_{\gamma^*\gamma}(Q^2), \quad (4)$$

using its Q^2 dependence near zero; $\Gamma^{\rm LT}_{\gamma^*\gamma}$ is the $\gamma^*\gamma$ decay width corresponding to a formation of the resonance from a longitudinal (virtual) photon and a transverse (real) photon. By substituting this expression into Eq. (3), we obtain

$$\frac{\mathrm{d}\sigma_{ee}(X)}{\mathrm{d}Q^2} = 4\pi^2 \frac{3}{M^2} 2 \frac{Q^2}{M^2} \epsilon \tilde{\Gamma}_{\gamma\gamma} 2 \left.\frac{\mathrm{d}^2 L_{\gamma^*\gamma}}{\mathrm{d}W \mathrm{d}Q^2}\right|_{W=M} \quad (5)$$

for $Q^2 \ll M^2$, where an extra factor of two comes from the difference in the number of spin degrees of freedom: the longitudinal component has one degree of freedom and the transverse component has two degrees of freedom in unpolarized incident photons. The quantity ϵ in Eq. (5) is the ratio $L_{\rm LT}/L_{\rm TT}$, where $L_{\rm LT}$ is the luminosity function for the production of one longitudinally polarized photon and one transversely polarized photon and $L_{\rm TT}$ is that of two transversely polarized photons. Using the Schuler-Berends-Gulik (SBG) model [6][30] for $q\bar{q}$-type axial-vector mesons, this can be extended to a higher Q^2 region [29] as

$$\frac{\mathrm{d}\sigma_{ee}(X)}{\mathrm{d}Q^2} = \tilde{\Gamma}_{\gamma\gamma} F(M, Q^2, \epsilon) \left.\frac{\mathrm{d}^2 L_{\gamma^*\gamma}}{\mathrm{d}W \mathrm{d}Q^2}\right|_{W=M}, \tag{6}$$

where

$$F(M, Q^2, \epsilon) = \frac{48\pi^2}{M^2} \frac{\frac{Q^2}{2M^2} + \epsilon}{\left(1 + \frac{Q^2}{M^2}\right)^3} \frac{Q^2}{M^2}, \tag{7}$$

accounting for the contributions from helicity 0 and 1.

To obtain the relation between the number of signal events and the decay width, $\tilde{\Gamma}_{\gamma\gamma}$, we use Eqs. (6) and (7) assuming the $X(3872)$ is a pure $c\bar{c}$ state [6]

$$\begin{aligned} N_{\rm sig} &= L_{\rm int} \mathcal{B}(X \to J/\psi\pi^+\pi^-) \mathcal{B}(J/\psi \to \ell^+\ell^-) \\ &\times \tilde{\Gamma}_{\gamma\gamma} \int_{Q^2_{\rm min}}^{Q^2_{\rm max}} \mathrm{d}Q^2 F(M, Q^2, \epsilon) \varepsilon_{\rm eff}(Q^2) \left.\frac{\mathrm{d}^2 L_{\gamma^*\gamma}}{\mathrm{d}W \mathrm{d}Q^2}\right|_{W=M}, \end{aligned} \tag{8}$$

where $\varepsilon_{\rm eff}(Q^2)$ is the Q^2-dependent reconstruction efficiency, $L_{\rm int}$ is the integrated luminosity, $\mathcal{B}(X \to J/\psi\pi^+\pi^-)$ is the branching fraction of the $X(3872)$ to $J/\psi\pi^+\pi^-$, and $\mathcal{B}(J/\psi \to \ell^+\ell^-) = 0.1193$ is the branching fraction of J/ψ to lepton pairs [25]. We estimate the reconstruction efficiency from MC, in which we model the $X(3872)$ decay as $X(3872) \to J/\psi\rho^0$ with $J/\psi \to \ell^+\ell^-$ and $\rho^0 \to \pi^+\pi^-$ and with all daughter particles isotropically distributed in the rest frames of their parents. The decay model via ρ is motivated by the measured invariant mass distributions [1, 31, 32]. It has a reconstruction efficiency 12% higher than that of non-resonantly produced $\pi^+\pi^-$; we include a 6% systematic uncertainty to account for this. The angular distribution of the decay products of the $X(3872)$ negligibly affects the reconstruction, as confirmed by simulating with an alternative model with decay angles of daughters from a $J^P = 1^+$ resonance with helicities 0 and 1. We estimate the efficiencies for our three center-of-mass beam energies—5.01, 5.29 and 5.43 GeV, corresponding to the $\Upsilon(2S)$, $\Upsilon(4S)$, and $\Upsilon(5S)$ resonance energies—and average the values weighted by their corresponding integrated luminosities. We also average over

the four detection modes given the two tagging charges (e^+ and e^-) and the two J/ψ decay modes (e^+e^- and $\mu^+\mu^-$). Figure 5 shows the result.

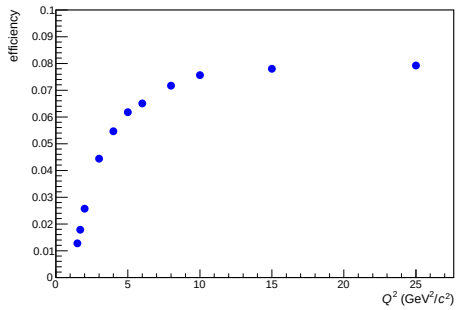

FIG. 5. Beam-energy-averaged reconstruction efficiency, $\varepsilon_{\rm eff}$, as a function of Q^2. Each data point has 13% systematic uncertainty.

The luminosity functions for our three beam energies are calculated as functions of Q^2 using TREPSBSS. We set $\epsilon = 1$ as a convention for the present application of Eq. (7)[6]. After performing the Q^2 integration in Eq. (8), from $Q^2_{\rm min} = 1.5$ GeV$^2/c^2$ to $Q^2_{\rm max} = 25$ GeV$^2/c^2$, we obtain

$$\tilde{\Gamma}_{\gamma\gamma}\mathcal{B}(X(3872) \to J/\psi\pi^+\pi^-) = (1.88 \pm 0.24)\ {\rm eV} \times N_{\rm sig}, \tag{9}$$

including the total systematic uncertainty from the integration.

The dominant systematic uncertainty on the product $\tilde{\Gamma}_{\gamma\gamma}\mathcal{B}(X \to J/\psi\pi^+\pi^-)$ is that on the reconstruction efficiency, primarily due to the differences between MC and data shown in Table I as effects due to selection criteria. The e^+e^- background uncertainty in the J/ψ selection, 7%, comes from the difference between MC and data in the e^+e^- background level. We estimate that the total systematic uncertainty is 13%.

From $N_{\rm sig}$, we determine

$$\tilde{\Gamma}_{\gamma\gamma}\mathcal{B}(X \to J/\psi\pi^+\pi^-) = 5.5^{+4.1}_{-3.8}\ ({\rm stat.}) \pm 0.7\ ({\rm syst.})\ {\rm eV}.$$

To place a limit on $\tilde{\Gamma}_{\gamma\gamma}$, we need $\mathcal{B}(X \to J/\psi\pi^+\pi^-)$. We derive an upper limit, using the measured products of B-meson decay branching fractions and the $X(3872)$ decay branching fractions, $\mathcal{B}(B^+ \to K^+X)\mathcal{B}(X \to J/\psi\pi^+\pi^-$ and other specific final states) [33]. With the measured lower limit [25, 31, 34], this gives $0.032 < \mathcal{B}(X \to J/\psi\pi^+\pi^-) < 0.061$ at the 90% C.L. Using the Feldman-Cousins method for three observed events and 0.11 background, we obtain $0.995 < N_{\rm sig} < 7.315$ at the 90% C.L. This, with Eq. (9), divided by $\mathcal{B}(X \to$

TABLE I. Systematic uncertainties on $\tilde{\Gamma}_{\gamma\gamma}\mathcal{B}(X \to J/\psi\pi^+\pi^-)$.

Item	Subitem	Uncertainty	Total
J/ψ	Electron and muon ID selections	4%	
	e^+e^- background	7%	
	J/ψ mass selection	1%	
Subtotal			8%
Tag	Electron ID selection	3%	
	γ radiation from $e^\pm$	$\sim$0%	
	p criterion	4%	
	$p^*_{\rm T}$ criterion	1%	
	Fake tag	0.3%	
Subtotal			5%
$M(\pi^+\pi^-)$ MC model in $X(3872)$ decay		6%	
Pion ID selections		3%	
$p^*_{\rm T}$-$E_{\rm obs}/E_{\rm exp}$ selection		4%	
$p^*_{\rm T}$ criterion		1%	
Missing p criterion		2%	
Back-to-back selection		2%	
Track finding		1.4%	
MC data size		0.6%	
Subtotal for efficiency systematics			13 %
Q^2 integration		1%	
Luminosity measurement		1.4%	
Luminosity function		3%	
$\mathcal{B}(J/\psi \to \ell^+\ell^-)$		0.4%	
Total			13%

$J/\psi\pi^+\pi^-$), gives the $\tilde{\Gamma}_{\gamma\gamma}$ range: 20-500 eV. This range is consistent with values predicted for the $c\bar{c}$ model [6, 8]. For non-$c\bar{c}$ models, we have to wait for improved calculations in the future.

No events consistent with $X(3915) \to J/\psi\pi^+\pi^-$ are observed. This, combined with the past measurements [9, 35], indicates there is no excess of G-parity-violating decays of $X(3915)$.

In summary, we find the first evidence for $X(3872)$ production in two-photon, $\gamma^*\gamma$, interactions. We observe three $X(3872)$ candidates with a significance of 3.2σ and an estimated yield of $2.9^{+2.2}_{-2.0}$ (stat.) ± 0.1 (syst.). From this, we obtain $\tilde{\Gamma}_{\gamma\gamma}\mathcal{B}(X(3872) \to J/\psi\pi^+\pi^-) = 5.5^{+4.1}_{-3.8}(\text{stat.}) \pm 0.7(\text{syst.})$ eV, using the Q^2 dependence expected from a $c\bar{c}$ meson model. With future advances in the calculations of $\tilde{\Gamma}_{\gamma\gamma}$ for non-$c\bar{c}$ states and the higher luminosities of Belle II, it is expected that this method will contribute to the clarification of the nature of the $X(3872)$.

We thank the KEKB group for excellent operation of the accelerator; the KEK cryogenics group for efficient solenoid operations; and the KEK computer group, the NII, and PNNL/EMSL for valuable computing and SINET5 network support. We acknowledge support from MEXT, JSPS and Nagoya's TLPRC (Japan); ARC (Australia); FWF (Austria); NSFC and CCEPP (China); MSMT (Czechia); CZF, DFG, EXC153, and VS (Germany); DST (India); INFN (Italy); MOE, MSIP, NRF, RSRI, FLRFAS project, GSDC of KISTI and KREONET/GLORIAD (Korea); MNiSW and NCN (Poland); MSHE, Agreement 14.W03.31.0026 (Russia); University of Tabuk (Saudi Arabia); ARRS (Slovenia); IKERBASQUE (Spain); SNSF (Switzerland); MOE and MOST (Taiwan); and DOE and NSF (USA).

[1] S.-K. Choi *et al.* (Belle Collaboration), Phys. Rev. Lett. **91**, 262001 (2003).

[2] R. Aaij *et al.* (LHCb Collaboration), Phys. Rev. Lett. **110**, 222001 (2013).

[3] R. Aaij *et al.* (LHCb Collaboration), arXiv: 2005.13419 [hep-ex] (2020).

[4] R. Aaij *et al.* (LHCb Collaboration), arXiv: 2005.13422 [hep-ex] (2020).

[5] The $X(3872)$ was searched for in two-photon interactions, before the spin-parity determination: S. Dobbs *et al.* (CLEO Collaboration), Phys. Rev. Lett. **94**, 032004 (2005).

[6] G. A. Schuler, F. A. Berends, and R. van Gulik, Nucl. Phys. **B 523**, 423 (1998).

[7] We use "electron" to stand for both electron and positron.

[8] T. Branz, R. Molina and E. Oset, Phys. Rev. **D 83**, 114015 (2011).

[9] S. Uehara *et al.* (Belle Collaboration), Phys. Rev. Lett. **104**, 092001 (2010).

[10] S. Kurokawa and E. Kikutani, Nucl. Instrum. and Methods Phys. Res., Sect. **A 499**, 1 (2003).

[11] T. Abe *et al.* (KEKB), Prog. Theor. Exp. Phys. **2013**, 03A001 (2013).

[12] A. Abashian *et al.* (Belle Collaboration), Nucl. Instrum. and Methods Phys. Res., Sect. **A 479**, 117 (2002).

[13] J. Brodzicka *et al.* (Belle Collaboration), Prog. Theor. Exp. Phys. **2012**, 04D001 (2012).

[14] M. Masuda *et al.* (Belle Collaboration), Phys. Rev. **D 93**, 032003 (2016).

[15] S. Uehara, KEK Report 96-11 (1996), arXiv: 1310.0157 [hep-ph].

[16] E. Barberio, B. van Eijk and Z. Was, Compt. Phys. Commun. **66**, 115 (1991).

[17] E. Barberio and Z. Was, Compt. Phys. Commun. **79**, 291 (1994).

[18] R. Brun *et al.*, CERN DD/EE/ 84-1 (1987).

[19] K. Hanagaki *et al.*, Nucl. Instrum. and Methods Phys. Res., Sect. **A 485**, 490 (2002).

[20] A. Abashian *et al.*, Nucl. Instrum. and Methods Phys. Res., Sect. **A 491**, 69 (2002).

[21] The various likelihood ratios are defined as $R_e = \mathcal{L}_e/(\mathcal{L}_e + \mathcal{L}_\pi)$, $R_\mu = \mathcal{L}_\mu/(\mathcal{L}_e + \mathcal{L}_\pi + \mathcal{L}_K)$, and $R_K = \mathcal{L}_K/(\mathcal{L}_K + \mathcal{L}_\pi)$, where $\mathcal{L}_x$ is the likelihood when the particle species x is assumed.

[22] E. Nakano, Nucl. Instrum. and Methods Phys. Res., Sect. **A 494**, 402 (2002).

[23] The e^+e^- center-of-mass quantities are indicated by asterisks.

[24] Recent measurements of the decay width show $\Gamma^{\rm BW}_{X(3872)} = 0.96^{+0.19}_{-0.18} \pm 0.21$ MeV [4] and $\Gamma^{\rm BW}_{X(3872)} = 1.39 \pm 0.24 \pm 0.10$ MeV [3].

[25] N. Tanabashi *et al.* (Particle Data Group), Phys. Rev. **D 98**, 030001 (2018), and 2019 update.

[26] C. Z. Yuan *et al.* (Belle Collaboration), Phys. Rev. Lett. **99**, 182004 (2007), Figure 1 shows $M(\ell^+\ell^-\pi^+\pi^-)$.

[27] G. J. Feldman and R. D. Cousins, Phys. Rev. **D 57**, 3873 (1998).

[28] M. Masuda *et al.* (Belle Collaboration), Phys. Rev. **D 97**, 052003 (2018).

[29] H. Aihara *et al.* (TPC/2γ Collaboration), Phys. Rev. **D 38**, 1 (1988).

[30] As a validation of the SBG model at higher Q^2, Ref. [28] provides measurements of single-tag to no-tag ratios for the $\gamma\gamma$ decay widths for χ_{c0} and χ_{c2}, which agree with the predictions of this model.

[31] S.-K. Choi *et al.* (Belle Collaboration), Phys. Rev. **D 84**, 052004 (2011).

[32] A. Abulencia *et al.* (CDF Collaboration), Phys. Rev. Lett. **96**, 102002 (2006).

[33] From $\mathcal{B}(B^+ \to K^+X)\mathcal{B}(X \to J/\psi\pi^+\pi^-) = (8.6 \pm 0.6) \times 10^{-6}$ and the sum over the measured products of the branching fractions, $\mathcal{B}(B^+ \to K^+X)\mathcal{B}(X \to J/\psi\pi^+\pi^-, J/\psi\gamma, \psi(2S)\gamma, D^0\bar{D}^0\pi^0, \bar{D^{*0}}D^0) = (1.4 \pm 0.4) \times 10^{-4}$, where we exclude $\bar{D}^{*0} \to \bar{D}^0\pi^0$, we obtain that $\mathcal{B}(X \to J/\psi\pi^+\pi^-) < 0.061$ using the Bayesian method at the 90% C.L. This limit is consistent with C. Li and C.-Z. Yuan, Phys. Rev. **D 100**, 094003 (2019).

[34] B. Aubert *et al.* (BaBar Collaboration), Phys. Rev. **D 77**, 111101 (2008).

[35] J. P. Lees *et al.* (BaBar Collaboration), Phys. Rev. **D 86**, 072002 (2012).